Ideal MHD stability limits of advanced tokamak plasmas and implications for the spherical torus.

J.E. Menard[1], D.A. Gates[1], S.C. Jardin[1], J. Manickam[1], S.A. Sabbagh[2], M.G. Bell[1], R.E. Bell[1], E.D. Fredrickson[1], S.M. Kaye[1], B.P. LeBlanc[1], R. Maingi[3], D. Mueller[1], M. Ono[1], F. Paoletti[2], Y.-K.M. Peng[3], D. Stutman[4], E.J. Synakowski[1], and the NSTX research team.
[1]*Princeton Plasma Physics Laboratory, Princeton, New Jersey*
[2]*Columbia University, New York, New York*
[3]*Oak Ridge National Laboratory, Oak Ridge, Tennessee*
[4]*Johns Hopkins University, Baltimore, Maryland*

(Dated: July 5, 2002)

Ideal magnetohydrodynamic stability limits of shaped tokamak plasmas with high bootstrap fraction are systematically determined as a function of plasma aspect ratio for the first time. For plasmas with and without wall stabilization of external kink modes, the computed limits are well described by a normalized beta parameter utilizing the total magnetic field energy density inside the plasma. Data from the National Spherical Torus Experiment is presented corroborating the utility of this definition of normalized beta in describing observed beta limits at very low aspect ratio and further indicates that ideal non-rotating plasma no-wall beta limits have been exceeded. The aspect ratio dependence of the computed beta limit indicates that the optimal aspect ratio for fusion power production in a normally conducting tokamak is at or above 1.6.

PACS numbers: 52.55.Fa, 28.52.Av

Introduction – The superconducting advanced tokamak [1, 2] is presently the leading candidate for producing an efficient magnetic fusion reactor. Alternative concepts such as the compact stellarator [3, 4] and spherical torus [5, 6] are also actively being studied as possible improvements to the advanced tokamak. The advanced tokamak (AT) and spherical torus (ST) reactor concepts share several features in common. Specifically, both rely on the neoclassical bootstrap current [7] to sustain nearly all of the plasma current and on stabilization of pressure-driven external kink modes to achieve sufficiently high beta (ratio of plasma kinetic pressure to magnetic pressure) to produce power efficiently. The AT and ST reactor concepts have been independently optimized for various physics and engineering constraints and arrive at notably different plasma aspect ratio and beta. This difference has motivated the present work which seeks to understand how the theoretical magnetohydrodynamic (MHD) stability limits of the AT and ST are linked. More generally, aspect ratio invariants (or near invariants) of advanced tokamak stability are sought. Two equilibrium regimes are treated in the following analysis. The first consists of a fully bootstrap-current-driven plasma utilizing a close-fitting conducting shell to stabilize external kink modes. The stability limits of this regime represent the maximum achievable beta of a tokamak at any aspect ratio given the present understanding of tokamak physics. The second regime consists of a plasma with a self-driven current fraction of 50% and no external kink stabilization. The stability limits of this regime have largely been experimentally realized in present-day tokamaks but have only recently been realized in relatively new ST experiments. Experimental results from strongly auxiliary-heated National Spherical Torus Experiment (NSTX) [8] plasmas are presented which highlight the significant difference between various definitions of beta. Further, it is shown that for a range of kink safety factor values the experimentally achieved beta values have exceeded theoretical limits computed in the absence of rotation and wall stabilization.

Advanced Tokamak Stability – The numerical methods and definitions used here for determining tokamak equilibrum and stability are well established and have been described previously [9]. To compute the highest achievable beta limit for the wall-stabilized self-sustaining advanced tokamak, several assumptions are made. The plasma boundary is assumed to be limited and D-shaped with a triangularity of 0.6-0.65, the self-driven current fraction is held above 99%, and kink modes with toroidal mode number below 8 are stabilized by a superconducting conformal wall positioned no closer than 10% of the plasma minor radius away from the plasma surface. Efficient calculation of the strength of wall stabilization in this work has been made possible through improvements to the PEST-II [10] code which allow the kink marginally-stable conformal wall position to be determined iteratively for a given equilibrium and toroidal mode number. All equilibria treated here are marginally stable to high-n ballooning modes and have a vanishing pressure gradient at the plasma boundary. The maximum plasma elongation is limited by the onset of n=1 kink modes which cannot be stabilized by the wall, and the n=0 vertical instability is assumed to be suppressed by a combination of the passive conducting shell and standard vertical po-

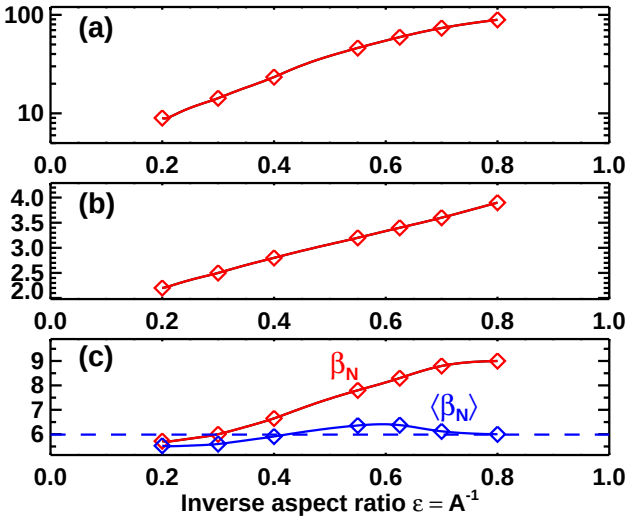

FIG. 1: (a) Toroidal beta, (b) plasma elongation, and (c) normalized toroidal and volume-average beta values versus inverse aspect ratio for the wall-stabilized fully self-sustained advanced tokamak.

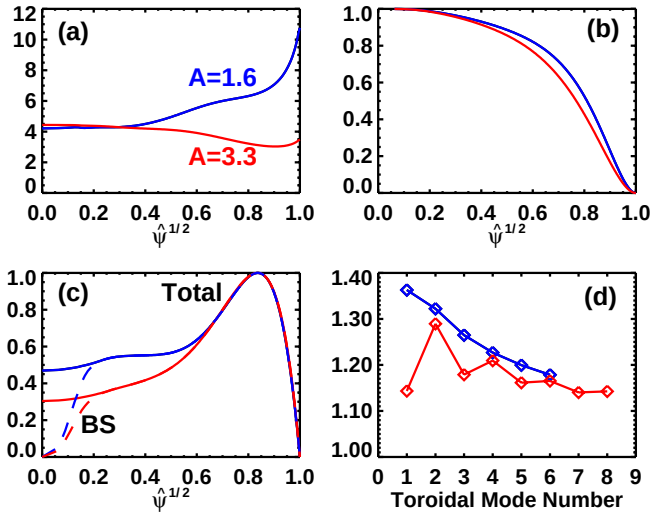

FIG. 2: (a) q (safety factor) profiles, (b) normalized pressure profiles, (c) normalized flux-surface-averaged parallel current density profiles, and (d) kink marginally-stable wall position divided by plasma minor radius for the A=1.6 and A=3.3 equilibria shown in Figure 1.

sition feedback methods. The normalized density and temperature profile functions are chosen to have similar peaking factors, and $Z_{ave} = 1.25$ and $Z_{eff} = 2$ are assumed in the specification of the collisionless bootstrap current density profile.

Figure 1 shows the theoretically computed maximum stable beta and elongation for wall-stabilized self-sustained tokamak plasmas. As seen in Figure 1a, the toroidal beta $\beta_t \equiv 2\mu_0\langle \mathrm{p}\rangle/\mathrm{B_{t0}}^2$ increases nearly an order of magnitude from 9% to 84% as the inverse aspect ratio ϵ is increased from 0.2 to 0.8. Figure 1b shows that the n=1 stability-limited elongation nearly doubles from 2.2 to 3.9 for the same range of aspect ratios. Figure 1c shows that the normalized toroidal beta $\beta_N \equiv \beta_\mathrm{t}(\%)\mathrm{aB_{t0}}/\mathrm{I_P(MA)}$ increases from 5.7 to 9.0. As shown in Ref. [9], the toroidal beta scales as $\beta_t \sim \sqrt{\epsilon}(1+\kappa^2){\beta_N}^2/f_{BS}$ implying that the explicit dependence of the beta limit on aspect ratio is relatively weak when bootstrap fraction is held fixed. Thus, the strong dependence of the elongation and normalized toroidal beta on aspect ratio are together responsible for most of the increase in toroidal beta with decreasing aspect ratio. Figure 1c also shows that the normalized volume-averaged beta $\langle\beta_N\rangle \equiv \beta_N \mathrm{B}_{t0}^2/\langle \mathrm{B}^2\rangle$ first utilized by Troyon [11] in parameterizing no-wall stability limits exhibits much smaller standard deviation (6% versus 18%) with aspect ratio relative to β_N and is an approximate stability invariant. These results suggest that the beta limit for the wall-stabilized self-sustaining advanced tokamak is $\langle\beta_N\rangle \approx 6$ nearly independent of aspect ratio.

The optimal profiles in the stability calculations discussed above are found to vary only slightly with aspect ratio with one notable exception. Figure 2a shows that the safety factor profile for A=1.6 is monotonically increasing as a function of minor radius (square root of the normalized poloidal flux), while for A=3.3 the q profile exhibits strongly reversed-shear. The shear changes sign from positive to negative near A=2.0, so this aspect ratio represents a possible natural dividing line between the spherical and standard tokamak. Figure 2b shows that the optimal pressure profiles are generally quite broad, and the pressure peaking factors $\mathrm{p}(0)/\langle \mathrm{p}\rangle$ are found to increase from 1.38 to 1.57 between A=1.25 and A=5.0. Figure 2c shows that both parallel current density profiles $\langle \vec{J}\cdot\vec{B}\rangle/\langle \vec{B}\cdot\nabla\phi\rangle$ are hollow and driven completely by the bootstrap effect except for a small region in the core. Finally, as shown in Figure 2d, for low aspect ratio there is a monotonic decrease in marginal wall position with increasing toroidal mode number. In contrast, for high aspect ratio the wall position can exhibit oscillations due the influence of individual mode rational surfaces associated with lower edge q and shear.

The very high beta regimes with fully self-driven current outlined in the previous section are theoretically achievable but have not yet been realized experimentally. The physical understanding of external kink stabilization utilizing rotation [12, 13] and active feedback [14] has improved significantly recently, but normalized beta values significantly above those attainable with optimized profiles without kink stabilization are not easily achieved. Further, the pressure profile control techniques required to realize the highest beta values in fully bootstrapped regimes are only beginning to be developed. These factors motivate an investigation of the aspect ratio dependence of the ideal beta limit for parameters routinely achieved in standard aspect ratio tokamaks but only recently achieved in relatively new ST devices.

In the following analysis, ideal beta limits are determined for equilibria with a fixed self-driven current frac-

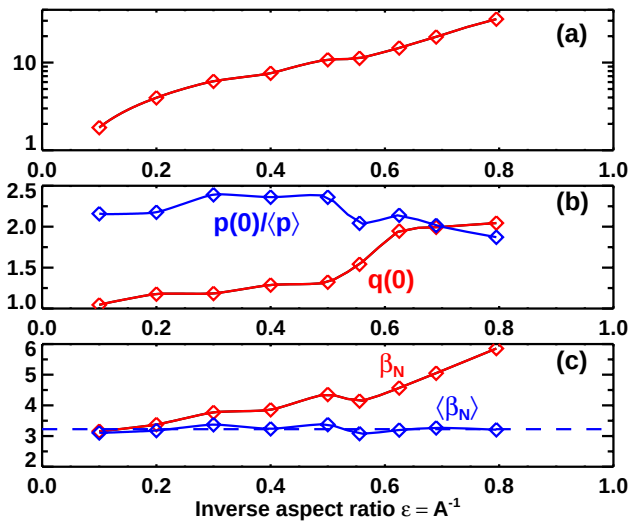

FIG. 3: (a) Toroidal beta, (b) pressure peaking and central safety factor, and (c) normalized toroidal and volume average beta values versus inverse aspect ratio for the 50% self-sustained advanced tokamak not utilizing wall stabilization.

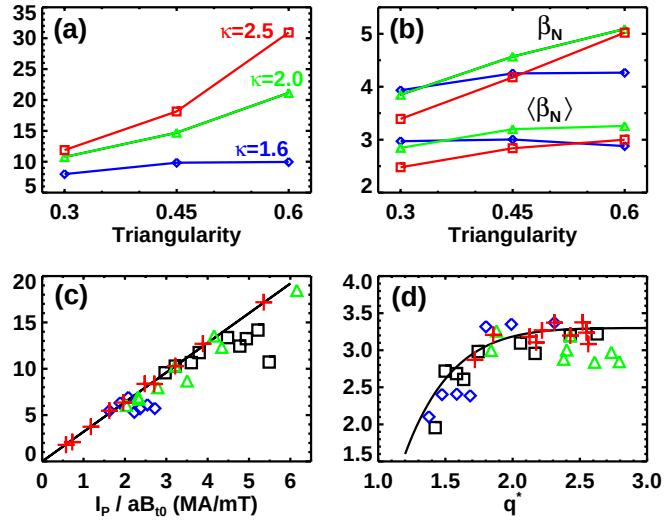

FIG. 4: (a) Marginally stable $\beta_t(\%)$ and (b) normalized beta values as a function of triangularity and elongation at 50% self-driven current fraction for aspect ratio A=1.6. (c) $\langle\beta\rangle$ versus I_P/aB_{t0} and (d) $\langle\beta_N\rangle$ versus kink safety factor for the aspect ratio, shape, and I_P scans performed for this study.

tion of 50%, which are marginally stable to ballooning modes and n=1-3 kink modes without wall stabilization, and have a fixed boundary shape with elongation $\kappa = 2.0$ and triangularity $\delta = 0.45$. For most aspect ratios treated, the optimization of the pressure and current profiles results in the equilibrium being simultaneously marginally stable to ballooning and n=1 kink modes, and all cases have no bootstrap current overdrive. With this set of constraints, Figure 3a again shows an order of magnitude increase in toroidal beta as the inverse aspect ratio is increased from 0.1 to 0.8. Figure 3b shows that the optimal pressure peaking is significantly higher when wall stabilization cannot be utilized and that there is a systematic decrease in the optimal peaking for $\epsilon > 0.5$. This figure also shows that the optimal central safety factor is approximately 2 for $\epsilon > 0.6$ and 1 to 1.3 for $\epsilon < 0.5$. Thus, for this optimization, A=1.8 is apparently a transitional aspect ratio lying between the spherical and standard tokamak. Finally, Figure 3c shows that the normalized toroidal beta increases from 3.15 to 5.85 between $\epsilon = 0.1$ and 0.8. In contrast, the normalized volume-averaged beta is again essentially independent of aspect ratio with a standard deviation of only 3% and mean value of 3.2.

The near invariance of $\langle\beta_N\rangle$ discussed above was obtained assuming fixed plasma shape and self-driven current fraction. Figure 4a shows that at A=1.6 with fixed self-driven current fraction = 50% the no-wall kink and ballooning marginally stable toroidal beta can vary as much as a factor of 4 depending on shaping. For these shape changes, Figure 4b shows that the normalized toroidal beta varies from 3.4 to 5, while the normalized volume-average beta values have only a 5% deviation from a mean value of 3.0 with the exception of the case with the lowest triangularity and highest elongation. Figure 4c plots $\langle\beta\rangle$ versus I_P/aB_{t0} for the aspect ratio scan of Figure 3 (crosses), the shape scan of Figure 4a (triangles), and an I_P scan for A=1.6 (squares) and A=3.3 (diamonds) at fixed $\kappa = 2.0$ and $\delta = 0.45$. As seen in the Figure, the solid line of $\langle\beta\rangle(\%) = 3.2\ I_P/aB_{t0}(\mathrm{MA/mT})$ represents an upper-bound for the beta limits found. For cases with $\langle\beta_N\rangle$ significantly below 3, it is found that $\langle\beta_N\rangle$ degrades rapidly as the kink safety factor $q^* \equiv \epsilon(1+\kappa^2)\pi aB_{t0}/\mu_0 I_P$ [9] is decreased below 2 for both A=1.6 and A=3.3, as shown in Figure 4d. This finding suggests that q^* may be a nearly aspect ratio invariant parameter for describing the dependence of profile-optimized stability limits on safety factor at high values of normalized current I_P/aB_{t0}, and further appears to be consistent with published experimental stability data [15, 16] for standard aspect ratio tokamaks.

NSTX stability and implications – Results from the previous section suggest that no-wall beta limits should be well described by $\langle\beta_N\rangle \approx 3.2$ except when q* is less than 2 and for highly elongated plasmas with low triangularity (see papers 90-93 in Ref. [15]). Recent machine improvements in the NSTX device now allow routine access to the H-mode [17] and its associated low pressure profile peaking ($p(0)/\langle p\rangle \approx 1.8$-$2.5$) predicted to be optimal for ideal MHD stability in the ST. As seen in Figure 5a, peak NSTX beta values computed with the EFIT equilibrium reconstruction code [18] clearly scale with I_P/aB_{t0} and have exceeded $\beta_t = 30\%$ with β_N values above 6 and $\langle\beta_N\rangle > 3$. Further, NSTX experimental $\langle\beta_N\rangle$ values plotted versus kink safety factor in Figure 5b exhibit the predicted degradation at low q^* shown by the black curve from Figure 4d. Both figures include plasmas with shape parameters ranging from A=1.27-1.5, κ=1.5-2.15, and δ=0.25-0.85. Importantly, H-mode

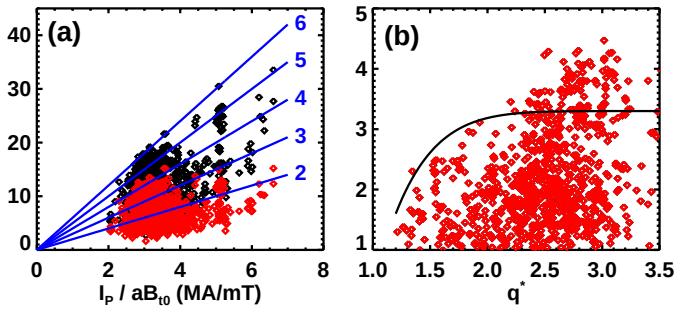

FIG. 5: (a) β_t (black) and $\langle\beta\rangle$ (red) (both in percent) at maximum stored energy for NSTX NBI-heated discharges above 600kA plotted versus normalized current. Constant normalized beta lines are shown in blue. (b) $\langle\beta_N\rangle$ versus kink safety factor q^* for the discharges from (a).

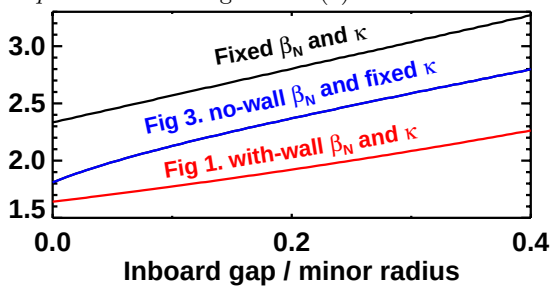

FIG. 6: Aspect ratio which maximizes fusion power production versus inboard plasma-TF coil separation normalized to plasma minor radius.

discharges with A=1.4-1.5 and κ=2 optimized to have very long ELM-free and sawtooth-free periods and q^* in the range of 2.5-3.0 have exceeded the theoretical no-wall limit $\langle\beta_N\rangle \approx 3.2$ by as much as 30% as seen in Figure 5b. Possible explanations include wall-stabilization of the pressure-driven kink mode [19] or shear stabilization of either kink or ballooning modes [20]. These discharges also reach poloidal beta values above 1.2 with n=2 and 3 mode activity present but do not appear to be limited by n=1 tearing modes as observed in MAST [21]. EFIT indicates q(0) > 2 for these discharges, but confirmation of elevated q awaits implementation of internal q profile diagnostics on NSTX.

Given the ability of NSTX plasmas to experimentally meet and exceed the highest theoretical ideal no-wall stability limits previously discussed, the stability results shown in Figures 1 and 3 can be used with increased confidence to estimate the optimum aspect ratio for DT fusion power production at fixed plasma major radius. For this optimization, the fusion power is assumed to scale as $\int p^2 dV$, the cost of external non-inductive current drive is ignored, and the maximum magnetic field strength at the toroidal field coil is held fixed. Figure 6 plots the optimal aspect ratio for fusion power production as a function of inboard plasma gap for three sets of stability assumptions. As evident from this figure, the increase in normalized toroidal beta (and elongation) with decreasing aspect ratio results in a significant reduction in the aspect ratio which maximizes fusion power production. Finally, parameterizations of these stability results could also be used to extend the range of validity of the stability scalings used in recent and more comprehensive reactor design calculations [22].

Summary – Systematic ideal stability calculations for advanced tokamak configurations scanning plasma aspect ratio, shape, and safety factor have been performed. The Troyon normalized beta value is found to best describe the calculated stability limits for all cases treated. The observed limits are $\langle\beta_N\rangle \approx 6$ for the wall-stabilized fully self-sustained tokamak and $\langle\beta_N\rangle \approx 3.2$ without wall stabilization with q^* above 2. NSTX peak plasma beta values are found to be at or above the theoretical maximum ideal no-wall limits and are thus far consistent with the expected behavior at low q^*. Using the computed stability limits, the aspect ratio for maximizing fusion power at fixed major radius is computed to be at or above A=1.6.

This research was supported by the United States Department of Energy under contract numbers DE-AC02-76CH03037 (PPPL), DE-AC05-00R22725 (ORNL), and grant numbers DE-FG02-99ER54524 (CU), DE-FG02-99ER54523 (JHU).

[1] S. Jardin *et al.*, Fus. Engin. and Design **38**, 27 (1997).
[2] C. Kessel, T. Mau, S. Jardin, and F. Najmabadi, Technical Report No. PPPL-3573, Princeton Plasma Physics Laboratory, (unpublished), submitted for publication to Fus. Eng. Design.
[3] S. Hirshman *et al.*, Phys. Rev. Lett. **80**, 528 (1998).
[4] M. C. Zarnstorff *et al.*, Plasma Phys. and Contr. Fus. **43**, 237 (2001).
[5] Y.-K. M. Peng and D. J. Strickler, Nucl. Fus. **26**, 769 (1986).
[6] R. D. Stambaugh, V. S. Chan, R. L. Miller, and M. J. Schaffer, Fus. Technol. **33**, 1 (1998).
[7] R. J. Bickerton, J. W. Connor, and J. B. Taylor, Nature Phys. Sci. **229**, 110 (1971).
[8] M. Ono *et al.*, Nucl. Fus. **40**, 557 (2000).
[9] J. E. Menard *et al.*, Nucl. Fus. **37**, 595 (1997).
[10] R. Grimm, R. L. Dewar, and J. Manickam, J. Comput. Phys. **49**, 94 (1983).
[11] F. Troyon *et al.*, Plasma Phys. and Contr. Fus. **26**, 209 (1984).
[12] A. Bondeson and D. J. Ward, Phys. Rev. Lett. **72**, 2709 (1994).
[13] A. M. Garofalo *et al.*, Phys. Rev. Lett. **82**, 3811 (1999).
[14] Y. Q. Liu and A. Bondeson, Phys. Rev. Lett. **84**, 907 (2000).
[15] E. Strait, Phys. Plasmas **1**, 1415 (1994).
[16] F. Hofmann *et al.*, Phys. Rev. Lett. **81**, 2918 (1998).
[17] R. Maingi *et al.*, Phys. Rev. Lett. **88**, 035003 (2002).
[18] S. A. Sabbagh *et al.*, Nucl. Fus. **41**, 1601 (2001).
[19] S. A. Sabbagh *et al.*, Phys. Plasmas **9**, 2085 (2002).
[20] F. Waelbroeck and L. Chen, Phys. Fluids B **3**, 601 (1991).
[21] R. J. Buttery *et al.*, Phys. Rev. Lett. **88**, 125005 (2002).
[22] C. P. C. Wong, J. C. Wesley, R. D. Stambaugh, and E. T. Cheng, Nucl. Fus. **42**, 547 (2002).